

Discovery of a Series of Indole-2 Carboxamides as Selective Secreted Phospholipase A₂ Type X (sPLA₂-X) Inhibitors

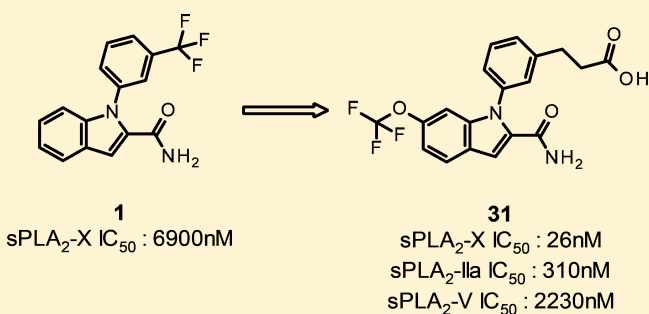
Laurent Knerr,^{*,†,Ⓜ} Fabrizio Giordanetto,^{*,†,Ⓜ} Peter Nordberg,[†] Daniel Pettersen,[†] Nidhal Selmi,[†] Hans-Georg Beisel,^{†,◆} Hannah de la Motte,^{†,□} Thomas Olsson,^{†,△} Tim D. J. Perkins,[†] Margareta Herslöf,[†] Åsa Månsson,^{†,▽} Mikael Dahlström,[†] Ingemar Starke,[†] Johan Broddefalk,[†] Gabrielle Saarinen,^{†,Ⓜ} Fredrik Klingegård,^{†,||} Eva Hurt-Camejo,[‡] Birgitta Rosengren,[§] Johan Brengdahl,^{||} Frank Jansen,[⊥] Mattias Rohman,^{||} Jenny Sandmark,[▽] Kenth Hallberg,^{▽,■} Tomas Åkerud,[▽] Robert G. Roth,[▽] and Marie Ahlqvist[#]

[†]Medicinal Chemistry, [‡]Translational Sciences, [§]Bioscience and [#]Drug Metabolism and Pharmacokinetics, Cardiovascular and Metabolic Diseases, IMED Biotech Unit, AstraZeneca, Gothenburg SE-431 89, Sweden

^{||}Reagents and Assay Development, [⊥]Mechanistic Biology and Profiling, and [▽]Structure and Biophysics, Discovery Sciences, IMED Biotech Unit, AstraZeneca, Gothenburg SE-431 89, Sweden

Supporting Information

ABSTRACT: In order to assess the potential of sPLA₂-X as a therapeutic target for atherosclerosis, novel sPLA₂ inhibitors with improved type X selectivity are required. To achieve the objective of identifying such compounds, we embarked on a lead generation effort that resulted in the identification of a novel series of indole-2-carboxamides as selective sPLA₂-X inhibitors with excellent potential for further optimization.



KEYWORDS: Secreted phospholipase A₂ type X, inhibitor, X-ray crystallography, atherosclerosis, coronary artery disease

Secreted phospholipases A₂ (sPLA₂s) are structurally conserved enzymes catalyzing the hydrolysis of glycerophospholipids at the *sn*-2 position, leading to the production of free fatty acids and lysophospholipids.¹ Accumulating evidence indicates that several sPLA₂ isoforms, namely, IIA (sPLA₂-IIA), sPLA₂-III, sPLA₂-V, and sPLA₂-X play significant, distinct, or overlapping roles in one or several steps of atherogenesis.² This led to the clinical testing of A-002 (varespladib methyl) (Figure 1), a nonselective inhibitor of sPLA₂-IIA, sPLA₂-V, and X isoforms, for the treatment of coronary artery

disease.³ Group X sPLA₂ (sPLA₂-X) is structurally related to other sPLA₂ isoforms, and among these, it is the most potent at hydrolyzing phosphatidylcholine, a highly abundant phospholipid at the cell surface and on lipoproteins.^{4,5} This enzyme is expressed in atherosclerotic lesions and peripheral blood cells.⁶ *In vitro* and *in vivo* studies have reported pro-atherogenic properties of sPLA₂-X comprising lipoprotein modifications leading to foam cell formation, reduced cell cholesterol efflux, altered immune cells maturation, and vascular cells proliferation.^{7–10} These effects indicate that sPLA₂-X is a potential novel therapeutic target for the treatment of cardiovascular diseases.² However, an *in vivo* study in a mouse model of atherosclerosis has shown that expression of sPLA₂-X in bone marrow cells limits the development of atherosclerosis.¹¹ Additionally, the VISTA-16 (Vascular Inflammation Suppression to Treat Acute Coronary Syndrome) phase III trial showed that administration of varespladib methyl did not reduce the occurrence of acute coronary syndrome (ACS) events but significantly increased the risk of nonfatal myocardial infarction.¹² These results could indicate that a broad spectrum sPLA₂ inhibitor may

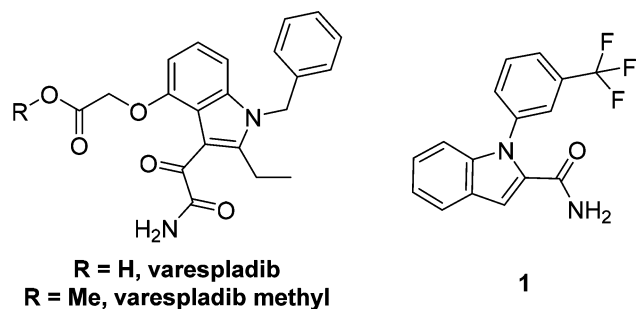


Figure 1. sPLA₂ inhibitor varespladib methyl, its active metabolite varespladib, and initial hit 1.

Received: December 4, 2017

Accepted: June 23, 2018

Published: June 23, 2018

be detrimental in atherosclerotic cardiovascular disease. Alternatively, novel sPLA₂ inhibitors with improved potency, safety, and selectivity would be required to demonstrate a therapeutic benefit in atherosclerotic conditions. The availability of isoform-selective sPLA₂ inhibitors could help dissecting the individual contribution of different sPLA₂ enzymes in pro- and antiatherogenic mechanisms. We therefore embarked on a discovery effort aiming at generating sPLA₂-X inhibitors¹³ possessing 30-fold selectivity over other sPLA₂ subtypes and suitable for oral administration. The lead generation part of this project will be described here.

A combination of NMR screening and high throughput screening (HTS) of the AstraZeneca compound collection was devised to identify chemical starting points with the potential to deliver selective inhibitors of sPLA₂-X (see [Supporting Information](#) for a more detailed description). This resulted in the identification of indole carboxamide **1** as a low micromolar inhibitor of sPLA₂-X ([Figure 1](#)).

A crystal structure of **1** bound to sPLA₂-X was solved and showed that the carboxamide group of **1** established three hydrogen bonds and one coordination bond with the protein and the catalytic calcium ion, respectively ([Figure 2](#)), similar to

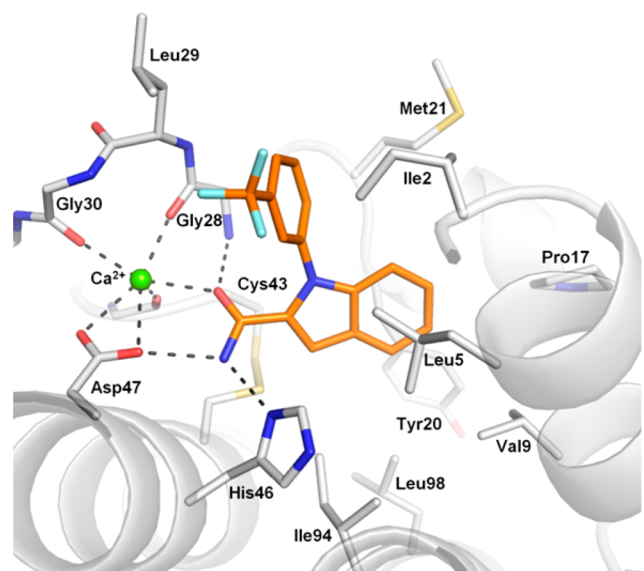


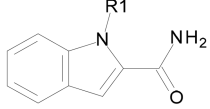
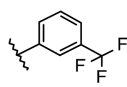
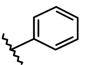
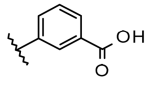
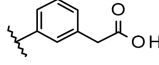
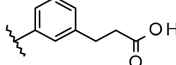
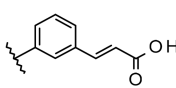
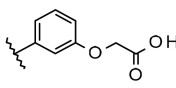
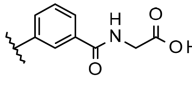
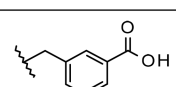
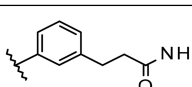
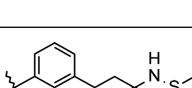
Figure 2. Crystal structure of sPLA₂-X in complex with compound **1** (orange). The amide of **1** forms three hydrogen bonds to the protein (2.7–3.1 Å) and one coordination bond to the calcium ion (2.5 Å), all marked by dashed lines.

analogous interactions reported in the literature,¹⁴ highlighting the importance of primary amides as warheads for sPLA₂ inhibition. The indole core of **1** occupies a hydrophobic pocket lined by residues Leu5, Val9, Pro17, Tyr20, Cys43, Ile94, and Leu98. Interestingly, this lipophilic pocket differs across sPLA₂ isoforms. In sPLA₂-IIa, the most closely related isoform to sPLA₂-X, Leu5, Val9, and Leu98 are replaced by Phe, Ile, and Phe, respectively ([Figure 2](#)). We hypothesized that these differences in side chain sizes could effectively result in a difference in pocket sizes, thus potentially offering a design manifold to improve sPLA₂ isoform selectivity by modifying/substituting the phenyl part of the indole core. The *meta*-trifluoromethyl phenyl group of **1** is involved in hydrophobic interactions with Ile2, Leu5, Gly28, Leu29, Tyr50, and Lys61.

Based on this structural framework, we set out to improve both the inhibitory potency and the selectivity versus the most widely abundant sPLA₂ isoforms IIa and V. Ligand efficiency

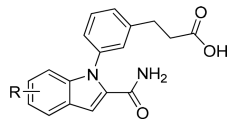
(LE) and ligand lipophilicity efficiency (LLE) were carefully monitored during this process to ensure that, despite the lipophilic nature of the binding pocket, lipophilicity and molecular properties would be kept in line with oral bioavailability potential. As a first step, we embarked on derivatizing the terminal *N*-aryl ring substituting the indole nitrogen atom of **1** with a view to establishing a second ligand interaction with the calcium ion. We reasoned this design hypothesis could have resulted in improved sPLA₂ inhibition while affording a more balanced physical chemical profile compatible with adequate solubility and metabolic stability by virtue of the envisioned polar chelating groups. Here, based on available data,^{14–18} special emphasis was placed on carboxylic acids/bioisosteres, as summarized in [Table 1](#). The unsubstituted *N*-phenyl-containing derivative (**2**) was essentially inactive. We noticed that, in a number of sPLA₂-X crystal structures available to our team, a water molecule or component of the crystallization buffer was found to coordinate the calcium ion in close proximity to the area occupied by the trifluoromethyl group of **1**. We therefore decided to focus on this position for introducing structural elements compatible with a second calcium interaction. Introduction of a carboxylic acid group in the *meta* position resulted in measurable inhibition of sPLA₂-X (**3**, [Table 1](#)). Atomic spacers between the aryl and carboxylic acid group improved the activity 3-fold for methylene (**4**) and 30-fold for the ethylene resulting in the first submicromolar sPLA₂-X inhibitor, endowed with high ligand and ligand lipophilicity efficiencies (**5**, [Table 1](#)). Based on this result and to further validate our modeling results, modification of the ethyl spacer by rigidification through unsaturation (**6**) or variation of the phenyl anchoring moiety using ether (**7**) or amide (**8**) groups was attempted but turned out to be poorly tolerated with seven to 27-fold loss of sPLA₂-X inhibitory activity. An initial attempt of functionalizing the indole core by *N*-benzylation instead of *N*-arylation proved counterproductive as well (**9**, [Table 1](#)). Replacement of the carboxylic acid group by a primary amide (**10**) yielded a complete loss of inhibition, while an acylsulfonamide bioisosteric element (**11**) was tolerated albeit with a 5-fold reduction in potency, indicating specific spatial and electronic restraints for the coordination of the calcium ion. Having identified **5** as a promising sPLA₂-X inhibitor, we assessed the importance of the indole system (see [Table S1](#) in the [Supporting Information](#)). Truncation of the indole to a pyrrole ring (**12**) highlighted the requirement of a bicyclic system for sPLA₂-X inhibition. Introduction of polarity using 7-azaindole (**13**) or imidazo[1,2-*a*]pyridine (**14**) scaffolds was not tolerated. Conservative changes using thienopyrrole cores (**15**, **16**) also resulted in total loss of inhibitory activity. Partial reduction of the indole core by saturation of the phenyl ring (**17**) was tolerated, although this reduced sPLA₂-X inhibition 6-fold. Based on these results, we resorted to using the indole scaffold of **5** as the basis for further molecular designs to explore the impact of indole substituents on both potency and selectivity. Systematic introduction of methyl groups (**18–21**, [Table 2](#)) indicated position 6 on the indole core as the most favorable for further optimization, due to the 4-fold sPLA₂-X inhibition improvement over **5** and the structural data available. Here, improvement of potency via introduction of electron withdrawing and lipophilic substituents such as chloride (**23**) and trifluoromethyl (**24**) yielded encouraging sPLA₂-X inhibitory activity when using high density lipoprotein (HDL) as a more disease-relevant sPLA₂-X substrate ([Table 2](#)). Further biological screening indicated that more voluminous substituents of electron donating

Table 1. sPLA₂-X Potency and Ligand Efficiencies for Compounds 1–11

			
	R1	sPLA ₂ -X IC ₅₀ (μM) ^{a,d}	LE/LLE ^b
	varespladib	0.041	
1		6.9	0.32/1
2		>30	<0.34/ND^c
3		29.1	0.29/4.5
4		10.3	0.30/4.8
5		0.99	0.35/5.6
6		23.6	0.27/4.2
7		26.9	0.27/4.5
8		7.2	0.28/5.1
9		20.7	0.29/4.6
10		>30	<0.26/<3.3
11		4.8	0.25/4.6

^aResults are mean of at least two experiments. Experimental errors within 20% of value [enzyme]. Substrate composition: 50 mg of 1-palmitoyl-2-oleoyl-*sn*-glycero-3-phosphocholine (Avanti Polar Lipids 850457P) in 1 mL of 4% NonidetP40 (USB) and 2% deoxycholic acid (Sigma D6750). ^bLigand efficiency (LE) is expressed in units of kcal·mol⁻¹ per non-hydrogen atom and calculated as $-RT \text{pIC}_{50}(\text{sPLA}_2\text{-X})/2.303 \times \text{heavy atom count}$ using $R = 0.001987 \text{ kcal}\cdot\text{mol}^{-1}\cdot\text{K}^{-1}$ and $T = 298 \text{ K}$. Ligand lipophilicity efficiency (LLE) calculated as $-\text{pIC}_{50}(\text{sPLA}_2\text{-X}) - \text{measured logD}_{7.4}$. ^cNot determined. ^dTop concentration tested: 30 μM.

Table 2. sPLA₂-X Potency and Ligand Efficiencies for Compounds 18–32

					
	R	sPLA ₂ -X (HDL) IC ₅₀ (μM) ^a	sPLA ₂ -IIa IC ₅₀ (μM) ^a	sPLA ₂ -V IC ₅₀ (μM) ^a	LE/LLE ^b
	varespladib	0.041 (0.15)	0.012	0.124	0.36/6.6
5	H	0.99	NA ^c	NA ^c	0.37/5.9
18	4-Me	0.83			0.35/5.3
19	5-Me	2.7			0.32/4.8
20	6-Me	0.23	NA ^c	NA ^c	0.38/5.8
21	7-Me	1.9	NA ^c	NA ^c	0.33/5.2
22	6-F	0.26	NA ^c	NA ^c	0.36/6.0
23	6-Cl	0.09 (1.1)	5.7	NA ^c	0.4/6.0
24	6-CF ₃	0.043 (0.48)	0.89	3.7	0.37/5.9
25	6-Et	0.17	4.4	NA ^c	0.37/5.5
26	6-cPr	0.16 (1.9)	2.3	>10	0.36/5.5
27	6-OMe	0.62	NA ^c	NA ^c	0.33/5.9
28	6-CH ₂ OH	2.8	NA ^c	NA ^c	0.3/5.6
29	6-CN	0.11 (0.99)	3.9	NA ^c	0.37/6.7
30	6-OCF ₂ H	0.068 (0.37)	3.6	NA ^c	0.36/6.2
31	6-OCF ₃	0.026 (0.27)	0.31	2.23	0.36/6.0
32	6-OCH ₂ CF ₃	0.093 (0.74)	>10	NA ^c	0.33/5.6

^aResults are mean of at least two experiments. Experimental errors within 20% of value [enzyme]. Substrate compositions (i) PC: 50 mg of 1-palmitoyl-2-oleoyl-*sn*-glycero-3-phosphocholine (Avanti Polar Lipids 850457P) in 1 mL of 4% NonidetP40 (USB) and 2% deoxycholic acid (Sigma D6750). (ii) HDL: HDL isolated from human plasma by ultracentrifugation was used as substrate. ^bLigand efficiency (LE) is expressed in units of kcal·mol⁻¹ per non-hydrogen atom and calculated as $-RT \text{pIC}_{50}(\text{sPLA}_2\text{-X})/2.303 \times \text{heavy atom count}$ using $R = 0.001987 \text{ kcal}\cdot\text{mol}^{-1}\cdot\text{K}^{-1}$ and $T = 298 \text{ K}$. Ligand lipophilicity efficiency (LLE) calculated as $-\text{pIC}_{50}(\text{sPLA}_2\text{-X}) - \text{measured logD}_{7.4}$. ^cNot active at highest tested concentration (30 μM).

nature (i.e., ethyl (25), cyclopropyl (26), and methoxy (27)) did not offer any advantages over methyl. Introduction of polarity via hydroxymethyl (28) and cyano (29) substituents did not result in any further potency gains. Based on these emerging structure–activity relationships, we targeted bulkier substituents with electron withdrawing character. Specifically, trifluoromethoxy (31) proved superior to difluoromethoxy (30) and 2,2,2-trifluoroethoxy (32) alternatives (Table 3).

The crystal structure of sPLA₂-X and 31 confirmed the bidentate calcium interaction by the carboxamide and carboxylic groups (Figure 3). The carboxylic acid of 31 that also forms an additional hydrogen bond to the main chain nitrogen of Gly30. The ethylene linker utilizes a narrow space defined by the side chains of Asp47, Tyr50, and Lys61. One side of the phenyl substituent is stacking against the main chains of Gly28 and Leu29. The trifluoromethoxy substituent is accommodated in a hydrophobic pocket with extensive van der Waals contacts (distances 3.6–4.0 Å) to the side chains of Ile2, Ala6, Pro17, Ile18, and Met21. The binding mode of the indole core was unaltered compared to 1, and as hypothesized, sequence comparison between sPLA₂-X, -IIa, and -V suggests that residues in the indole binding pocket are likely to be determinants for

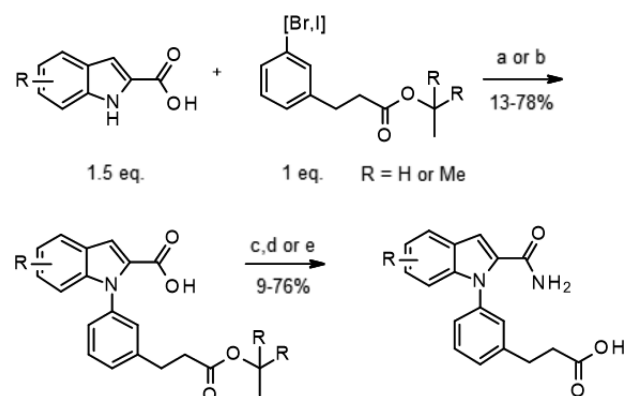
Table 3. Profiling of Compound 31^a

solubility (pH = 7.4) (μM)	98	
Caco-2 P_{app} (10^{-6} cm/s)	18.8	
human hepatocytes Cl_{int} ($\mu\text{L}/\text{min}/10^{-6}$ cells)	1.7	
sPLA ₂ -X IC_{50} (μM)	0.026	
sPLA ₂ -X mouse IC_{50} (μM)	0.096	
sPLA ₂ -IIa IC_{50} (μM)	0.31	
sPLA ₂ -V IC_{50} (μM)	2.23	
pharmacokinetics	rat	dog
dose i.v./p.o. ($\mu\text{mol}/\text{kg}$)	1/4	1/-
CL (mL/min/kg)	9.1	0.75
AUC ($\mu\text{M}\cdot\text{h}$)	1.84/11	8.78/-
V_{dss} (L/kg)	2.54	0.44
F (%)	100	

^aSee Supporting Information for experimental details

isoform selectivity (Figure 3A) by preventing the indole core from adopting the same binding mode, as reflected by the lower affinity of 31 for these isoforms (11- and 85-fold reduced potency to sPLA₂-X, respectively, Table 3).

While some close derivatives possessed better selectivity profiles (e.g., 30 and 32), 31 demonstrated improved lipolytic activity of sPLA₂-X on HDL (IC_{50} : 270 nM) and was therefore profiled further. Compound 31 did not display any significant binding to a large panel of biological targets and no significant inhibition of ion channels, enzymes, and transporters that

Scheme 1. General Synthesis of Indole-2 Carboxamides Derivatives^a

^aReagents and conditions: (a) $\text{Cu}(\text{OAc})_2$ (1 equiv), DBU (3 equiv), DMSO, μw , 140–150 °C; (b) CuI (0.2 equiv), piperidine-2-carboxylic (0.4 equiv), K_2CO_3 (3 equiv), DMF, 110 °C; (c) NH_4Cl (3 equiv), TBTU (1.5 equiv), DIEA (9 equiv), DMF, rt; (d) 4 M HCl in 1,4-dioxane, rt; (e) LiOH, THF, water, rt.

might be related to toxicity (Table 3). While the aqueous solubility and passive permeability of 31 were adequate, its *in vitro* metabolic stability was suboptimal, and this readily translated in sufficient oral bioavailability but high unbound clearance. These properties made 31 inadequate as a tool compound for

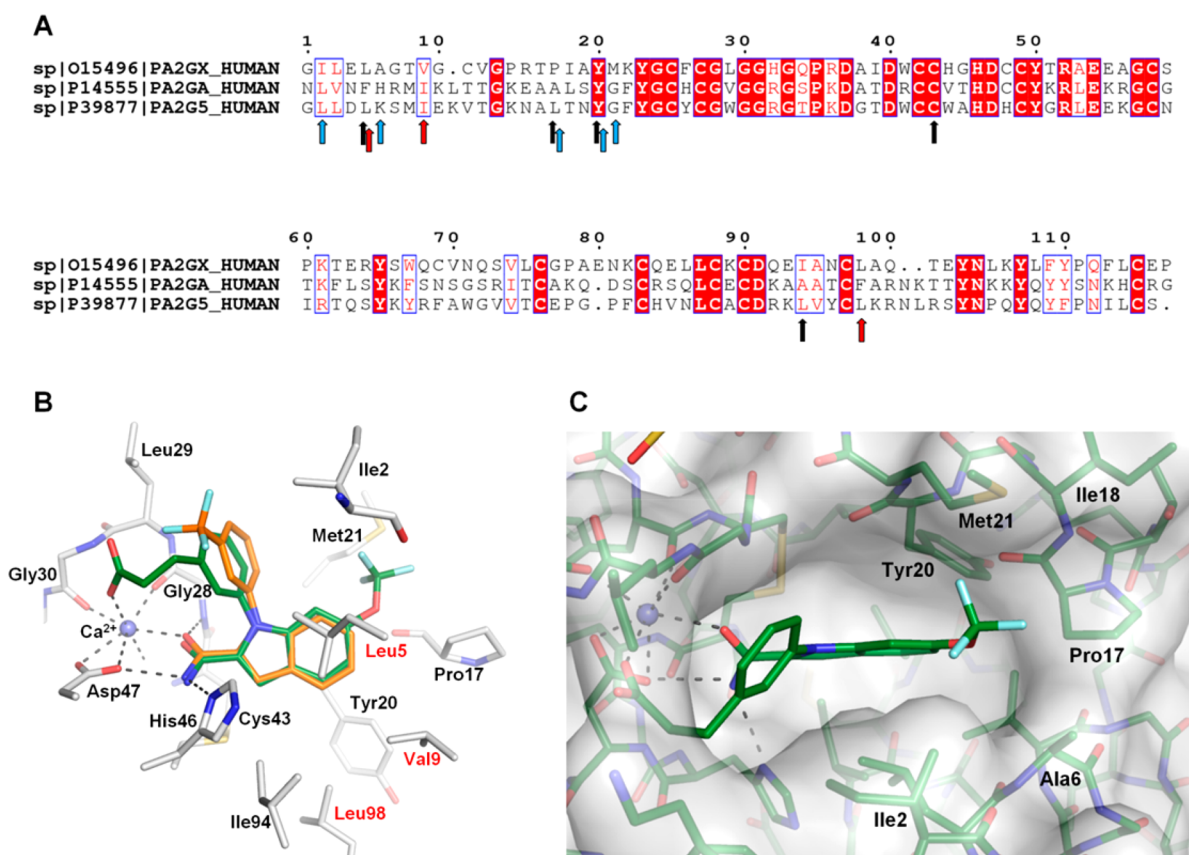


Figure 3. (A) Sequence alignment of mature sPLA₂-X (top), -IIa (middle), and -V (bottom). Black arrows mark residues that interact with the indole core. Blue arrows indicate residues that make up the hydrophobic pocket that harbors the trifluoromethoxy moiety. Red arrows highlight residues predicted to be determinants of sPLA₂ isoform selectivity. (B) Superposition of crystal structures of sPLA₂-X in complex with 1 (orange) and 31 (green). The structure shows that the carboxyl group of 31 forms the second interaction to the calcium ion. Three residues are marked in red (Leu5, Val9, and Ile94), as they are predicted to be responsible for isoform selectivity. (C) Crystal structure of sPLA₂-X in complex with 31. Residues lining the lipophilic pocket that harbors the trifluoromethoxy moiety are labeled.

in vivo evaluation due to too high doses required to cover IC₅₀ and IC₉₀ but offered clear avenues for further optimization.

The indole 2-carboxamides derivatives were efficiently prepared by liquid phase parallel synthesis using the approach described in Scheme 1. Starting from commercially available or readily accessible¹⁹ indole-2-carboxylic acids, the *N*-arylation was performed using two different copper based methods.^{20,21} The intermediate acids were then converted to primary amides before final removal of the *tert*-butyl ester protecting group. This synthetic sequence produced only modest to good overall yields but proved robust enough for the rapid generation of arrays of diverse derivatives presented here.

In summary, starting from the indole carboxamide hit **1**, a series of structure-based, medicinal chemistry explorations resulted in the identification of derivative **31**, a novel sPLA₂-X inhibitor with favorable properties for further investigation. The optimization of its selectivity and *in vivo* pharmacokinetic profile toward sPLA₂-X-centric, preclinical proof of concept studies in animals is detailed in the Companion paper.

■ ASSOCIATED CONTENT

📄 Supporting Information

The Supporting Information is available free of charge on the ACS Publications website at DOI: 10.1021/acsmchemlett.7b00505.

Experimental details, synthesis, assay protocols, and X-ray crystallographic statistics (PDF)

Accession Codes

PDB code for the X-ray crystal structure described in this study has been deposited in the Protein Data Bank under the accession codes 5OW8 and 5OWC.

■ AUTHOR INFORMATION

Corresponding Authors

* (L.K.) Tel: +46 317065788. E-mail: laurent.knerr@astrazeneca.com.

* (F.G.) Tel: +1(212) 478 0822. E-mail: fabrizio.giordanetto@DEShawResearch.com.

ORCID

Laurent Knerr: 0000-0002-4810-8526

Fabrizio Giordanetto: 0000-0001-9876-9552

Present Addresses

○ (F.G.) D.E. Shaw Research, 120 W 45th Street, New York, New York 10036, United States.

◆ (H.-G.B.) Medivir AB, SE-141 22 Huddinge, Sweden.

□ (H.d.l.M.) RISE Research Institutes of Sweden Division Bioeconomy, SE-417 56 Gothenburg, Sweden.

△ (T.O.) Gothenburg University, SE-405 30 Gothenburg, Sweden.

▼ (Å.M.) Alfa Laval Lund AB, SE-226 55 Lund, Sweden.

○ (G.S.) SCA Hygiene products AB, SE-851 88 Stockholm, Sweden.

‡ (F.K.) SciLifeLab, Drug Discovery & Development Platform, SE-171 21 Solna, Sweden.

■ (K.H.) SARomics Biostructures, SE-223 63 Lund, Sweden.

Notes

The authors declare no competing financial interest.

■ ACKNOWLEDGMENTS

The authors would like to acknowledge the support of the Structure Analysis and Separation Science group of AstraZeneca Gothenburg.

■ ABBREVIATIONS USED

sPLA₂, secreted phospholipase 2; VISTA, Vascular Inflammation Suppression to Treat Acute Coronary Syndrome; HTS, high throughput screening; ACS, acute coronary syndrome; PC, phosphatidylcholine; HDL, high density lipoprotein; LE, ligand efficiency; LLE, lipophilicity ligand efficiency; P_{app}, apparent permeability; Cl_{int}, intrinsic clearance; i.v., intravenous; p.o., per oral; CL, clearance; AUC, area under curve; Vd_{ss}, steady state volume of distribution; F, oral bioavailability; DBU, 2,3,4,6,7,8,9,10-octahydropyrimido[1,2-*a*]azepine; DMSO, dimethyl sulfoxide; DMF, dimethylformamide; TBTU, 2-(1*H*-benzo[*d*][1,2,3]triazol-1-yl)-1,1,3,3-tetramethylisouronium tetrafluoroborate; DIEA, diisopropylethylamine

■ REFERENCES

- (1) Murakami, M.; Taketomi, Y.; Miki, Y.; Sato, H.; Yamamoto, K.; Lambeau, G. Emerging roles of secreted phospholipase A2 enzymes: the 3rd edition. *Biochimie* **2014**, *107*, 105–113.
- (2) Rosenson, R. S.; Hurt-Camejo, E. Phospholipase A2 enzymes and the risk of atherosclerosis. *Eur. Heart J.* **2012**, *23*, 2899–2909.
- (3) Rosenson, R. S.; Fraser, H.; Trias, J.; Hislop, C. Varespladib methyl in cardiovascular disease. *Expert Opin. Invest. Drugs* **2010**, *10*, 1245–1255.
- (4) Kokotou, M. G.; Limnios, D.; Nikolaou, A.; Psarra, A.; Kokotos, G. Inhibitors of phospholipase A2 and their therapeutic potential: an update on patents (2012–2016). *Expert Opin. Ther. Pat.* **2017**, *27*, 217–225.
- (5) Pan, Y. H.; Yu, B. Z.; Singer, A. G.; Ghomashchi, F.; Lambeau, G.; Gelb, M. H.; Jain, M. K.; Bahnson, B. J. Crystal structure of human group X secreted phospholipase A2. Electrostatically neutral interfacial surface targets zwitterionic membranes. *J. Biol. Chem.* **2002**, *277*, 29086–29093.
- (6) Pruzanski, W.; Lambeau, G.; Lazdunski, M.; Cho, W.; Kopilov, J.; Kuksis, A. Hydrolysis of minor glycerophospholipids of plasma lipoproteins by human group IIA, V and X secretory phospholipases A2. *Biochim. Biophys. Acta, Mol. Cell Biol. Lipids* **2007**, *1736*, 5–19.
- (7) Jönsson-Rylander, A. C.; Lundin, S.; Rosengren, B.; Pettersson, C.; Hurt-Camejo, E. Role of secretory phospholipases in atherogenesis. *Curr. Atheroscler. Rep.* **2008**, *10*, 252–259.
- (8) Karabina, S. A.; Brochériou, I.; Le Naour, G.; Agrapart, M.; Durand, H.; Gelb, M.; Lambeau, G.; Ninio, E. Atherogenic properties of LDL particles modified by human group X secreted phospholipase A2 on human endothelial cell function. *FASEB J.* **2006**, *20*, 2547–2549.
- (9) Ishimoto, Y.; Yamada, K.; Yamamoto, S.; Ono, T.; Notoya, M.; Hanasaki, K. Group V and X secretory phospholipase A(2)s-induced modification of high-density lipoprotein linked to the reduction of its antiatherogenic functions. *Biochim. Biophys. Acta, Mol. Cell Res.* **2003**, *1642*, 129–138.
- (10) Atout, R.; Karabina, S. A.; Dollet, S.; Carreras, M.; Payré, C.; André, P.; Lambeau, G.; Lotteau, V.; Ninio, E.; Perrin-Cocon, L. Human group X secreted phospholipase A2 induces dendritic cell maturation through lipoprotein-dependent and -independent mechanisms. *Atherosclerosis* **2012**, *222*, 367–374.
- (11) Pruzanski, W.; Kopilov, J.; Kuksis, A. Hydrolysis of lipoproteins by sPLA2's enhances mitogenesis and eicosanoid release from vascular smooth muscle cells: Diverse activity of sPLA2's IIA, V and X. Pruzanski W, Kopilov J, Kuksis A. *Prostaglandins Other Lipid Mediators* **2016**, *122*, 64–68.
- (12) Nicholls, S. J.; Kastelein, J. J.; Schwartz, G. G.; Bash, D.; Rosenson, R. S.; Cavender, M. A.; Brennan, D. M.; Koenig, W.; Jukema, J. W.; Nambi, V.; Wright, R. S.; Menon, V.; Lincoff, A. M.; Nissen, S. E. VISTA-16 Investigators. Varespladib and cardiovascular events in patients with an acute coronary syndrome: the VISTA-16 randomized clinical trial. *JAMA* **2014**, *311*, 252–262.
- (13) Dennis, E. A.; Cao, J.; Hsu, Y. H.; Magriotti, V.; Kokotos, G. Phospholipase A₂ Enzymes: Physical Structure, Biological Function,

Disease Implication, Chemical Inhibition, and Therapeutic Intervention. *Chem. Rev.* **2011**, *111*, 6130–6185.

(14) Schevitz, R. W.; Bach, N. J.; Carlson, D. G.; Chirgadze, N. Y.; Clawson, D. K.; Dillard, R. D.; Draheim, S. E.; Hartley, L. W.; Jones, N. D.; Mihelich, E. D.; Olkowski, J. L.; Snyder, D. W.; Sommers, C.; Wery, J. P. Structure-based design of the first potent and selective inhibitor of human non-pancreatic secreted phospholipase A₂. *Nat. Struct. Mol. Biol.* **1995**, *2*, 458–465.

(15) Dillard, R. D.; Bach, N. J.; Draheim, S. E.; Berry, D. R.; Carlson, D. G.; Chirgadze, N. Y.; Clawson, D. K.; Hartley, L. W.; Johnson, L. M.; Jones, N. D.; McKinney, E. R.; Mihelich, E. D.; Olkowski, J. L.; Schevitz, R. W.; Smith, A. C.; Snyder, D. W.; Sommers, C. D.; Wery, J.-P. Indole inhibitors of human nonpancreatic secretory phospholipase A₂. 1.Indole-3-acetamides. *J. Med. Chem.* **1996**, *39*, 5119–5136.

(16) Dillard, R. D.; Bach, N. J.; Draheim, S. E.; Berry, D. R.; Carlson, D. G.; Chirgadze, N. Y.; Clawson, D. K.; Hartley, L. W.; Johnson, L. M.; Jones, N. D.; McKinney, E. R.; Mihelich, E. D.; Olkowski, J. L.; Schevitz, R. W.; Smith, A. C.; Snyder, D. W.; Sommers, C. D.; Wery, J.-P. Indole inhibitors of human nonpancreatic secretory phospholipase A₂. 2.Indole-3-acetamides with additional functionalities. *J. Med. Chem.* **1996**, *39*, 5137–5158.

(17) Dillard, R. D.; Bach, N. J.; Draheim, S. E.; Berry, D. R.; Carlson, D. G.; Chirgadze, N. Y.; Clawson, D. K.; Hartley, L. W.; Johnson, L. M.; Jones, N. D.; McKinney, E. R.; Mihelich, E. D.; Olkowski, J. L.; Schevitz, R. W.; Smith, A. C.; Snyder, D. W.; Sommers, C. D.; Wery, J.-P. Indole inhibitors of human nonpancreatic secretory phospholipase A₂. 2.Indole-3-glyoxamides. *J. Med. Chem.* **1996**, *39*, 5159–5175.

(18) Smart, B. P.; Oslund, R. C.; Walsh, L. A.; Gelb, M. H. The first potent inhibitor of mammalian group X secreted phospholipase A₂: elucidation of sites for enhanced binding. *J. Med. Chem.* **2006**, *49*, 2858–2860.

(19) Nazaré, M.; Schneider, C.; Lindenschmidt, A.; Will, D. W. A Flexible, Palladium-catalyzed indole and azaindole synthesis by direct annulation of chloroanilines and chloroaminopyridines with ketones. *Angew. Chem., Int. Ed.* **2004**, *43*, 4526–4528.

(20) Guo, X.; Rao, H.; Fu, H.; Jiang, Y.; Zhao, Y. An inexpensive and efficient copper catalyst for N-arylation of amines, amides and nitrogen-containing heterocycles. *Adv. Synth. Catal.* **2006**, *348*, 2197–2202.

(21) Huang, H.; Yan, X.; Zhu, W.; Liu, H.; Jiang, H.; Chen, K. Efficient copper-promoted N-arylations of aryl halides with amines. *J. Comb. Chem.* **2008**, *10*, 617–619.